Kinetic and Thermodynamic Studies of the Disproportionation of Hydrogen Peroxide by Dimanganese(II,II) and -(II,III) Complexes of a Bridging Phenolate Ligand[‡]

Lionel Dubois,[a] Dao-Feng Xiang,[a] Xiang-Shi Tan,[a] and Jean-Marc Latour*[a]

Keywords: Manganese / Catalase / H_2O_2 disproportionation / Kinetics

The dimanganese(II,II) complexes $[Mn_2(L)(OAc)_2(CH_3OH)](ClO_4)$ (**1a**) and $[Mn_2(L)(OBz)_2(H_2O)](ClO_4)$ (**1b**) as well as the dimanganese(II,III) complex $[Mn_2(L)(OAc)_2(CH_3OH)](ClO_4)_2$ (**2a**), where HL is the asymmetric phenol ligand 2-[bis(2-pyridylmethyl)aminomethyl]-6-{[(benzyl)(2-pyridylmethyl)amino]methyl}-4-methylphenol, react with hydrogen peroxide in acetonitrile solution. The initial reaction rates and their temperature and acid/base dependencies were investigated by monitoring the dioxygen evolution. These studies revealed a first-order dependence on both the catalyst and H_2O_2 and a strong influence of the carboxylate. Electrospray ionisation mass spectrometry as well as EPR and UV/Vis spectroscopy were used to monitor the reaction catalysed by **2a**. The same bis(μ-oxo)dimanganese(III,IV) and (μ-oxo)dimanganese(II,III) active species as found for **1a** were detected in the catalytic medium. The EPR spectra recorded during the catalase-like reaction revealed the accumulation of the magnetically uncoupled dimanganese(II,III) precursor of the active bis(μ-oxo)dimanganese(III,IV) species which dominates the spectra in the case of **1a**. This difference can be attributed to the different pH conditions generated by the reaction and reflects differences in the initiation phases for the two catalysts. Overall, the kinetic and thermodynamic studies of H_2O_2 disproportionation by these dimanganese complexes are fully consistent with the mechanism deduced from our previous extensive spectroscopic studies.

Introduction

Although it is a product of aerobic respiration, hydrogen peroxide is potentially toxic since its reduction produces the highly deleterious hydroxyl radical. To prevent formation of HO· and related oxidative stress, cells possess very efficient enzymatic machineries in which the catalase enzymes play an essential role.[1,2] These enzymes eliminate H_2O_2 by means of its disproportionation into harmless dioxygen and water. Most of these enzymes are haemoproteins but a few of them of bacterial origin[3–5] possess a dimanganese active site.[6,7] The two manganese atoms are triply bridged by the carboxylate group of a glutamate and two water-derived ligands, as revealed by the crystallographic studies of the enzymes from *Thermus thermophilus*[8] and *Lactobacillus plantarum*.[9]

Very limited information is available on their mechanism of action. Biochemical[10] and spectroscopic[11] studies have shown that during catalysis, the carboxylate-capped Mn_2O_2 diamond core shuttles between the oxidation states $Mn^{II}Mn^{II}$ and $Mn^{III}Mn^{III}$. However, the fast kinetics of the enzymatic reaction ($k_{cat} \approx 10^5$ s^{-1})[8] and the fact that the oxidised and the reduced forms both react with the same substrate (H_2O_2) have precluded a precise description. As a consequence, most mechanistic proposals have been based on studies of biomimetic compounds.[12–14] The most detailed of these studies were performed on complexes of ligands involving either alkoholates[14,15] or phenolates[13,16] which stabilise the dimanganese unit by providing it with an internal bridge. Depending upon the Mn ligands, all oxidation states of the pair from $Mn^{II}Mn^{II}$ to $Mn^{IV}Mn^{IV}$ have been implicated in the catalysis. In the case of dimanganese complexes of pentadentate bis(aminoalkylimino)phenol ligands, the involvement of oxomanganese(IV) species has been demonstrated by Okawa et al.[16,17] through the observation, in DMF, of a characteristic vibronically split electronic absorption of the $Mn^{IV}(O)$ unit. On the other hand, Nishida et al. provided EPR evidence of the formation of a bis(μ-oxo)dimanganese(III,IV) species in the reaction of hydrogen peroxide with dimanganese complexes of heptadentate hexaaminophenols but did not establish definitely whether this species is a catalytic intermediate or a mere by-product.[18]

As part of our continuing interest in the physical properties and reactivity of dimanganese compounds,[19] we reported the synthesis of the dimanganese(II,II) complexes

[a] Laboratoire de Physicochimie des Métaux en Biologie, Unité Mixte de Rechereche CEA-CNRS-Université Joseph Fourier UMR 5155, Département Réponse et Dynamique Cellulaires, CEA-Grenoble,
38054 Grenoble Cedex 9, France
Fax: +33-43878-3462
E-mail: Jean-Marc.Latour@cea.fr
[‡] Binuclear Manganese Compounds of Potential Biological Significance, 3. Part 2: Ref.[21]

$[Mn_2(L)(OAc)_2(CH_3OH)](ClO_4)$ (**1a**) and $[Mn_2(L)(OBz)_2(H_2O)](ClO_4)$ (**1b**) derived from the asymmetric phenolate ligand 2-{[bis(2-pyridylmethyl)amino]methyl}-6-{[(benzyl)-(2-pyridylmethyl)amino]methyl}-4-methylphenol (HL, Scheme 1).[20] We also showed that the hydrogen peroxide disproportionation induced by these complexes involves two intermediates, namely a (μ-oxo)dimanganese(II,III) species $[Mn_2(L)(OAc)(O)]^+$ and a bis(μ-oxo)dimanganese(III,IV) complex $[Mn_2(L)(OAc)(O)_2]^+$ which were characterised by a combination of electrospray ionisation mass spectrometry (ESI-MS) and EPR spectroscopy.[21] In addition, we described the independent synthesis of the bis(μ-oxo)dimanganese(III,IV) complex and its characterisation by X-ray absorption spectroscopy and we showed that the initial reaction of *tert*-butyl hydroperoxide (and probably H_2O_2 also) with the dimanganese(II,II) complexes is a one-electron oxidation to their dimanganese(II,III) analogue.[21] These results are summarised in Scheme 2.

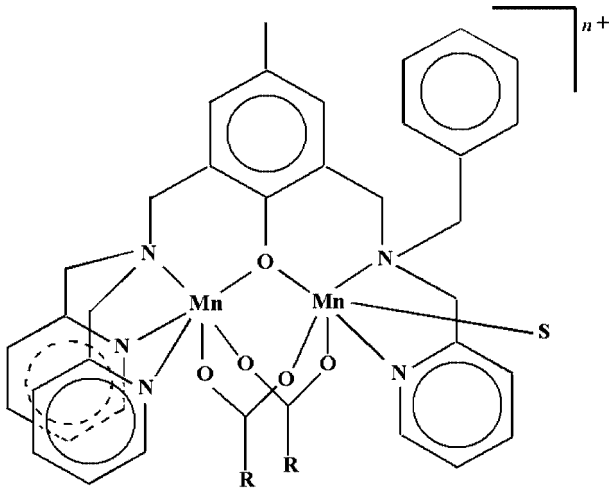

1a: R = Me, **S** = CH_3OH, n = 1
1b: R = Ph, **S** = H_2O, n = 1
2a: R = Me, **S** = H_2O, n = 2

Scheme 1. Complexes used in this study.

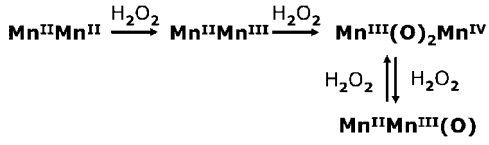

Scheme 2. Overall mechanism of the disproportionation of H_2O_2 by **1a**.

In the present article, we report kinetic and thermodynamic studies of the reaction of H_2O_2 with complexes **1a** and **1b** and the analogous dimanganese(II,III) compound $[Mn_2(L)(OAc)_2(H_2O)](ClO_4)_2$ (**2a**).[20] In addition, spectroscopic monitoring of the reaction of H_2O_2 with **2a** shows that the same intermediates are formed, therefore providing a consistent mechanistic picture for all complexes.

Results

Solvent Influence

Many different solvents were used in previous studies of the catalase-like reaction. In a few cases, solvent effects on the rate of dioxygen evolution were considered but the observed effects were found to depend on the catalyst.[18,23–25] It was also reported that even the mechanism of the reaction can change between DMF and acetonitrile.[18] These observations from the literature prompted us to investigate the solvent influence on the kinetics of dioxygen evolution upon reaction of H_2O_2 with **1a**. Figure 1 illustrates the data obtained at 0 °C in DMF, methanol and acetonitrile. In DMF, the reaction was very slow (0.012 mL min^{-1}) and only a small part (ca. 10%) of hydrogen peroxide was disproportionated. In methanol and acetonitrile, the reaction was faster (1.3 and 1.2 mL min^{-1}, respectively) and H_2O_2 was fully disproportionated. Although the initial rates of reaction are very similar, the reaction in methanol slowed down as it approached completion which is possibly due to the limited stability of the catalyst. For this reason, all subsequent measurements were performed in acetonitrile.

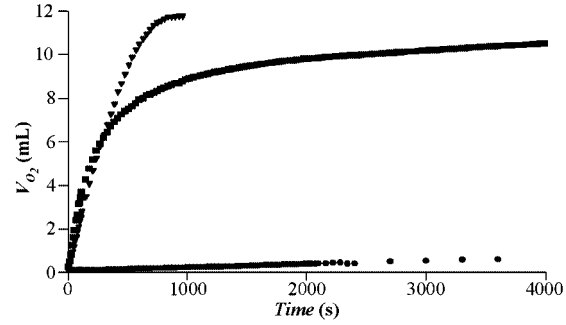

Figure 1. Time dependence of dioxygen evolution upon reaction of **1a** with H_2O_2 in different solvents: methanol (■), acetonitrile (▼) and DMF (●); [**1a**] = 1.0 mM, [H_2O_2] = 460 mM, T = 0 °C.

Comparison of the Catalysts – Stability

The activities of the different catalysts **1a**, **1b** and **2a** were studied under the same conditions as above and the kinetic results are illustrated in Figure 2. The most active catalyst was **2a** with an initial rate of O_2 evolution of 9 mL min^{-1} which can be compared with 1.2 and 0.9 mL min^{-1} for **1a** and **1b**, respectively. In each case, H_2O_2 underwent quantitative disproportionation. At the end of the reaction, the addition of another aliquot of 460 equiv. of hydrogen peroxide gave rise to a new evolution of dioxygen. In the case of **1a**, the rate increased from 1.2 mL min^{-1} for the first H_2O_2 batch to 3.45 mL min^{-1} for the second and 4.5 mL min^{-1} for the third. A sharp decrease in the rate of 2.0 and 0.2 mL min^{-1} was noted for the fourth and the fifth batches, respectively. In the case of **2a**, the rate of O_2 evolution was divided by a factor of 1.8 for the second addition and continued to decrease for the third and the fourth additions where the initial rate became very small (a lag phase was observed in this case).

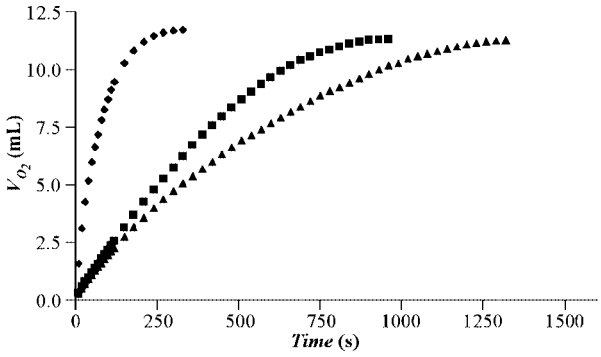

Figure 2. Time dependence of dioxygen evolution upon reaction of H_2O_2 with **1a** (■), **1b** (▼) and **2a** (♦) in acetonitrile; [catalyst] = 1.0 mM, [H_2O_2] = 460 mM, T = 0 °C.

Order of the Reaction

The order of the reaction with respect to the catalyst and hydrogen peroxide was investigated. In the case of **1a**, Figure 3 and Figure 4 show the influence of the complex and hydrogen peroxide concentrations on the reaction rate, respectively. After the initial rate determination, the curve of the Ln(initial rate) = f(concentration) gave a slope of 1.16 (r^2 = 0.998) with respect to the catalyst concentration and 1.12 (r^2 = 0.988) for hydrogen peroxide. It is worth noting that at low H_2O_2 concentrations ([H_2O_2] ≤ 115 mM), an initiation phase was observed over a period of ca. 100 s. In the case of **2a**, the slopes of the curve of the Ln(initial rate) = f(concentration) were 1.17 (r^2 = 0.991) and 0.95 (r^2 = 0.99998) for the catalyst and the hydrogen peroxide concentrations, respectively. Interestingly, no lag phase was detected whatever the H_2O_2 concentration. These results indicate that for **1a** and **2a**, the reaction follows a first-order dependence on both the hydrogen peroxide and the catalyst concentrations.

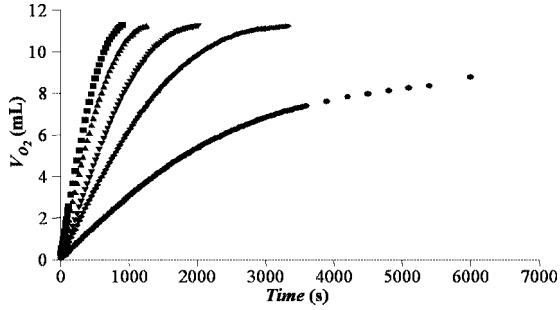

Figure 3. Time dependence of dioxygen evolution upon reaction of H_2O_2 with different concentrations of **1a** in acetonitrile: 1 mM (■), 0.8 mM (▼), 0.6 mM (▲), 0.4 mM (♦), 0.2 mM (●); [H_2O_2] = 460 mM, T = 0 °C.

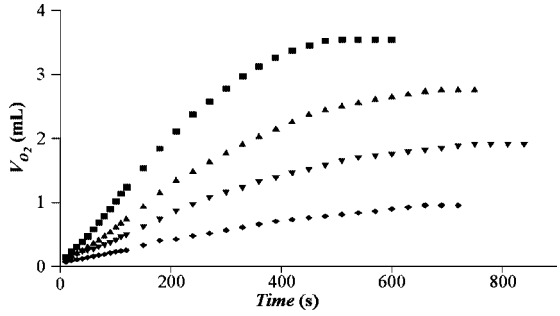

Figure 4. Time dependence of dioxygen evolution upon reaction of **1a** with different concentrations of H_2O_2 in acetonitrile: 115 mM (■), 86 mM (▼), 57 mM (▲), 29 mM (♦); [**1a**] = 1 mM, T = 0 °C.

Temperature Dependence

The determination of the thermodynamic parameters of the catalase-like reaction for the complexes **1a**, **1b** and **2a** was carried out by investigating the rate of dioxygen evolution at different temperatures over the range of –30 °C to +30 °C. After the initial rate determination, the curves Ln(initial rate) = $f(1/T)$ were plotted (Figure 5). For every catalyst, linear regression analysis proved satisfactory thereby indicating that the Arrhenius law is obeyed in all cases. The linear regression analysis provided the activating energy E_a and the preexponential factor k_0 and these parameters are summarised in Table 1. It is noteworthy that the complexes follow a trend in activation energy (**2a** > **1a** > **1b**) which parallels their activities. In other words, the highest activation energy is associated to the most active catalyst (**2a**). This observation contradicts the general view that the higher activity of a catalyst corresponds to a lower activating energy. It follows that the preexponential term k_0 is indeed the dominant factor.

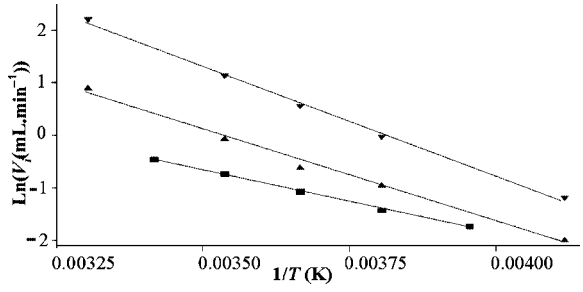

Figure 5. Temperature dependence of the initial rate of the catalase-like reaction in the form of the curve Ln(initial rate) vs. $1/T$ for **1a** (▼), **1b** (■) and **2a** (▲) in acetonitrile; [catalyst] = 1.0 mM, [H_2O_2] = 460 mM.

Table 1.Activation energies and preexponential factors for the reactions of **1a**, **1b** and **2a** with H_2O_2 in acetonitrile.

Catalyst	E_a [kJ mol^{-1}]	ln(k_0)	r^2
2a	35 ± 1	25.2 ± 0.5	0.992
1a	29 ± 1	22.0 ± 0.6	0.997
1b	20.0 ± 0.5	16.2 ± 0.2	0.998

Effect of Acid and Base Addition

In order to further assess the large differences in the abilities of **1a** and **1b** to disproportionate hydrogen peroxide, we decided to study the effect of acid and base addition on

the reaction rate. Figure 6 shows the effect, on the initial reaction rate in the case of **1a**, upon addition of perchloric acid or triethylamine. Upon addition of triethylamine, the rate increased and this effect reached a maximum at 3 equiv. (per complex) at which point the rate was 3 times higher. A more important effect was observed upon addition of 1 equiv. of perchloric acid and at this concentration the rate of dioxygen evolution was 7 times higher (4.2 mL min^{-1}) than in the absence of perchloric acid. Moreover, it is worth noting that, at this point, the rate is very close to that measured for **2a** (4.5 mL min^{-1} under the same conditions). Further addition of perchloric acid caused a decrease of the initial rate. For **2a**, no change was observed after addition of perchloric acid while addition of base induced its disproportionation into Mn^{II} and $Mn^{III}Mn^{IV}$ species (see below) as shown by EPR spectroscopy.

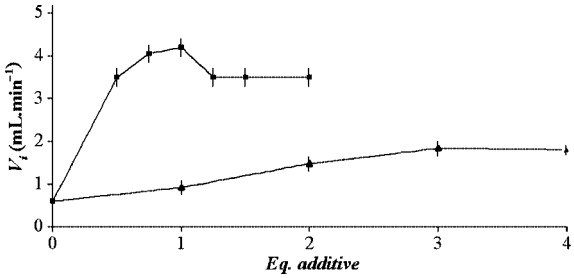

Figure 6. Effect of acid and base addition in the rate of the catalase-like reaction of **1a**: addition of triethylamine (▼), addition of perchloric acid (■).

Spectroscopic Monitoring of Hydrogen Peroxide Disproportionation by 2a

We have previously reported spectroscopic investigations of the mechanism of the reaction of hydrogen peroxide with **1a** and **1b**. We completed this study by monitoring the same reaction for **2a** by combining spectroscopic (UV/Vis, EPR) and mass spectrometric experiments.

UV/Vis Monitoring

When **2a** was treated with hydrogen peroxide in acetonitrile, its characteristic visible spectrum with maxima at 380, 485 and 627 nm[20] disappeared very rapidly (ca. 30 s.) and was replaced by three poorly resolved absorptions at 460, 550 and 630 nm. These absorptions are the signature of a bis(μ-oxo)$Mn^{III}Mn^{IV}$ complex[26] and were similarly observed previously and assigned to the active species in the disproportionation of H_2O_2 by **1a** and **1b**.[21] This spectrum was observed during the whole reaction and tended to disappear at times longer than 5 min.

EPR Monitoring

Figure 7 shows the EPR spectra recorded during the reaction of **2a** with H_2O_2. The initial spectrum (Figure 7a) consists of a large featureless signal between 150 mT and 500 mT with a characteristic poorly resolved 6-line signal superimposed on the central line, as already described.[20] This 6-line signal departs from that of the solvated Mn^{2+} ion and is characteristic of a Mn^{2+} centre bound to the ligand. After addition of H_2O_2 (460 mM, Figure 7b), the signal of **2a** disappeared rapidly (ca. 1 min) and was replaced by a well-resolved 6-line spectrum centred near 350 mT (g = 2). On both the high- and low-field sides of this signal, another weak signal could be detected also with a 16-line pattern which corresponds to a bis(μ-oxo)$Mn^{III}Mn^{IV}$ complex. At longer times (Figure 7c), these two signals decreased in intensity and were replaced by a new poorly resolved 6-line signal at 350 mT (g = 2). After ca. 30 min (Figure 7d), this last signal was the only one observed.

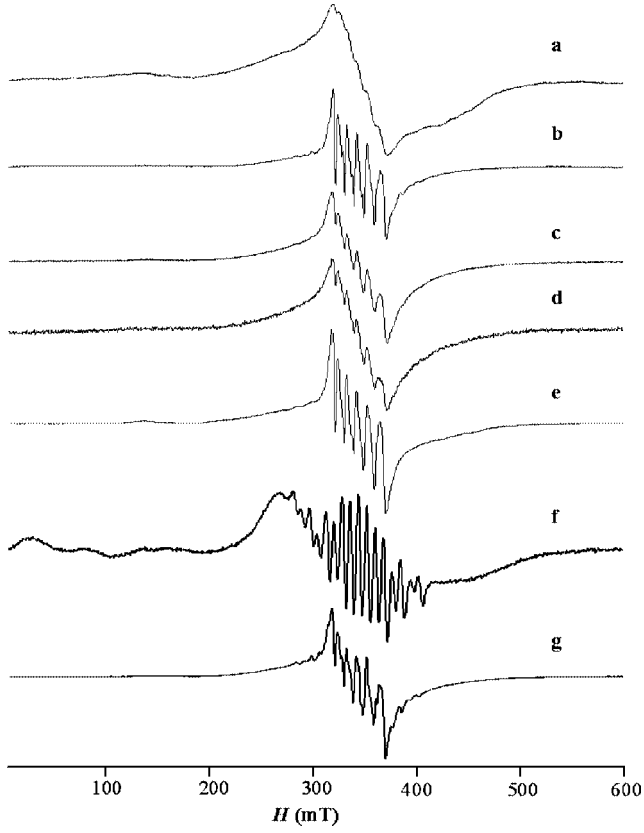

Figure 7. EPR spectra of the reaction of **2a** in acetonitrile with H_2O_2 and after addition of perchloric acid or triethylamine. Spectra a–d: reaction times 0, 1, 8 and 30 min; reaction conditions: [**2a**] = 1 mM, [H_2O_2] = 460 mM, T = –40 °C; spectrum e: **2a** + 1 equiv. perchloric acid; spectrum f: **2a** + 1 equiv. triethylamine; spectrum g: **1a** + 1 equiv. percloric acid + 460 equiv. H_2O_2. Reaction conditions [**1a**] = 1 mM, [H_2O_2] = 460 mM, T = 0 °C.

To further substantiate the effect of addition of acid or base to an acetonitrile solution of **2a**, its EPR spectrum was recorded in the presence of 1 equiv. of perchloric acid (Figure 7e). This spectrum possesses a better resolved 6-line signal centred at 350 mT (g = 2) which is completely different from that of **2a**. This spectrum is very similar to that of **1a** + 1 equiv. of perchloric acid (see Figure 4a in ref.[21]). The spectrum shown in Figure 7f was recorded after addition of 1 equiv. of triethylamine to **2a**. It consists of two signals, one with a 16-line pattern centred at 350 mT (g = 2) corresponding to a bis(μ-oxo)$Mn^{III}Mn^{IV}$ complex. The second one, composed of several transitions between 0 and 5500 G is characteristic of **1a**.[20] These results indicate that

2a is not stable in a basic medium and disproportionates into **1a** and a bis(μ-oxo)$Mn^{III}Mn^{IV}$ derivative. Spectrum 7 g was recorded during the reaction of **1a** with H_2O_2 after addition of 1 equiv. of perchloric acid. We can notice than this spectrum is very close to that of **2a** without perchloric acid (Figure 7b).

Mass Spectrometry Monitoring

To obtain a better characterisation of the reaction medium during the reaction of **2a** with hydrogen peroxide, it was monitored by ESI-MS. The results obtained are reported in Figure 8. The starting compound **2a** (Figure 8a) appeared in the form of 3 peaks at *m/z* = 854.8, 756.2 and 378.1 which correspond, respectively, to $[Mn^{II}Mn^{III}(\mu\text{-L})(\mu\text{-OAc})_2](ClO_4)]^+$, $[Mn^{II}Mn^{II}(\mu\text{-L})(\mu\text{-OAc})_2]^+$ and $[Mn^{II}Mn^{III}(\mu\text{-L})(\mu\text{-OAc})_2]^{2+}$. The second ion at *m/z* = 756 was formed by reduction of the starting material (or other related species) during the ionisation process and this can be confirmed by its absence in the corresponding EPR spectrum.[20] After addition of hydrogen peroxide (Figure 8b), new peaks appeared at *m/z* = 713.1, 729.2 and 742.3. All these signals were also observed during the reaction of **1a** with hydrogen peroxide[21] and labelling experiments enabled us to assign them to the two intermediates $[Mn^{II}Mn^{III}(\mu\text{-L})(\mu\text{-O})(\mu\text{-OAc})]^+$ and $[Mn^{III}Mn^{IV}(\mu\text{-L})(\mu\text{-O})_2(OAc)]^+$, and the oxidation product $[Mn^{II}Mn^{II}(\mu\text{-L})(\mu\text{-OAc})(\mu\text{-HCOO})]^+$, respectively. After ca. 17 min, the starting compound had been fully consumed as revealed by the spectrum depicted in Figure 8c showing that the peaks of the initial complex had disappeared.

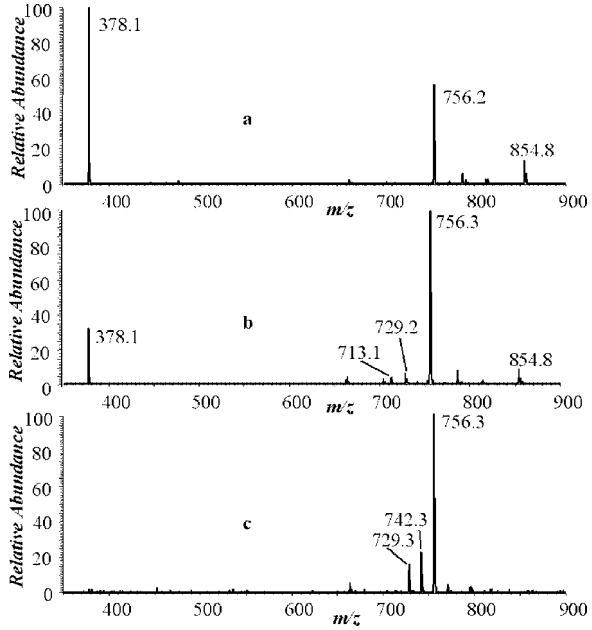

Figure 8. ESI-MS spectra of the reaction of **2a** with H_2O_2 in acetonitrile: spectra a–c: reaction times 0, 1 and 17 min; reaction conditions [**2a**] = 0.6 mM, $[H_2O_2]$ = 460 mM, *T* = –40 °C.

Discussion

Scheme 2 summarises the overall mechanism of H_2O_2 disproportionation by **1a** which emerged from our previous investigations of the reaction by a combination of UV/Vis, EPR, X-ray absorption spectroscopy and ESI mass spectrometry.[21] This mechanism involves an initiation phase in which **1a** is oxidised to the dimanganese(II,III) state with cleavage of the phenoxo bridge. A 6-line EPR signal centred at *g* = 2 is associated with this species. This compound can be viewed as the precursor to the catalytic species since it is further oxidised to the active bis(μ-oxo)dimanganese(III,IV) complex. In the catalase-like reaction, this complex oxidises H_2O_2 and is transformed into the (μ-oxo)dimanganese(II,III) species which is then able to reduce H_2O_2 to water. The present kinetic and thermodynamic studies of dioxygen evolution are fully consistent with this mechanistic scheme. In particular, a lag phase extending over ca. 100 s can be observed at low H_2O_2 concentrations in the case of **1a**. This lag phase more than likely corresponds to the required oxidation process to generate the precursor of the active species. Consistently, no lag phase was observed for **2a** or for **1a** at higher H_2O_2 concentrations. The present kinetic and thermodynamic studies provide a few observations which can valuably improve the understanding of the mechanism.

Firstly, we observed that on the first three successive additions of H_2O_2, the reaction rate of **1a** increased and eventually approached that of **2a**, while the latter did not show such a rate increase. This can be explained if the initiation process is slower than the disproportionation reaction. If this were the case, the disproportionation would start developing before all **1a** had entered the catalytic cycle. Successive additions would therefore bring more of **1a** into the active form. This view is supported by the observation that the less reactive **1b** persists longer than **1a** in the catalytic medium.[21]

Secondly, the kinetic measurements show that the initial rate of the catalase-like reaction is dependent on the nature of the bridging carboxylates. A similar observation was made by Okawa et al.[16,27,28] This result may indicate that at least one of the carboxylate groups remains in the coordination sphere of the active species. This conclusion is perfectly consistent with the results of our previous ESI-MS analyses of **1a** and **1b** which indicated the presence of one carboxylate in both active species.

Thirdly, the thermodynamic analysis of the reaction revealed similar trends (**2a** > **1a** > **1b**) in the activation energies and the preexponential terms. This trend in activation energy is opposite to the reaction efficiency but it is noteworthy that it parallels the bond strengths between the carboxylate ligands and the catalysts. It may then reflect the need to dissociate a carboxylate during the catalysis to make a coordination site available to hydrogen peroxide.

ESI-MS monitoring of the reaction of **2a** with H_2O_2 has shown that the bis(μ-oxo)$Mn^{III}Mn^{IV}$ and the (μ-oxo)Mn^{II}-Mn^{III} intermediates are involved as in the case of **1a**. Nevertheless, the EPR spectra recorded during the course of the reaction were dominated by the 6-line signal of the precursor. It is worth noting that such a species was transiently formed upon reaction of **1a** with H_2O_2.[21] Protonation experiments coupled with EPR spectroscopy showed that the same 6-line EPR spectrum can be obtained upon addition

of 2 equiv. of $HClO_4$ to **1a** or 1 equiv. to **2a**. This enhanced proton sensitivity of **2a** was attributed to the fact that its Mn^{II}–$O_{phenoxo}$ bond is significantly elongated (2.245 Å) and weakened with respect to the same bonds in **1a** (2.105–2.107 Å)[20] and therefore more susceptible to break in solution. This cleavage of the phenoxide bridge makes the dimanganese unit appear as the individual ions: an EPR-silent Mn^{III} and a mononuclear Mn^{II} with a 6-line signature. The influence of protonation on the reactivity experiments supports this view. Firstly, the rate of the catalase-like reaction of **1a** + 1 equiv. of perchloric acid is very close to that of **2a** without perchloric acid. Secondly, the EPR spectrum recorded during the catalase-like reaction of **1a** + 1 equiv. of perchloric acid and **2a** without perchloric acid are very similar and include a dominating contribution of the precursor (6-line signal at $g \approx 2$) and traces of a bis(μ-oxo)-$Mn^{III}Mn^{IV}$ complex (16-line signal at $g \approx 2$). It appears then that a unique mechanism is likely to be in operation for **1a** and **2a** but the different EPR signatures observed during the catalase-like reaction may reflect different proportions of EPR active species present in solution. Indeed, in the case of **1a**, the EPR spectrum is dominated by the 16-line signal of the active bis(μ-oxo)$Mn^{III}Mn^{IV}$ intermediate and the characteristic EPR signal of **1a** slowly disappears during the reaction. In contrast, in the case of **2a**, the spectrum of the precursor dominates and that of the active bis(μ-oxo)$Mn^{III}Mn^{IV}$ intermediate appears weak. This difference may have its origin in the different proton sensitivities of the starting complexes reinforced by the chemical processes required to form the active bis(μ-oxo)$Mn^{III}Mn^{IV}$ intermediate. Indeed, in the case of **1a**, the reaction requires $^3/_2$ H_2O_2 molecules and generates a single H^+ [Equation (1)].

$$Mn^{II}Mn^{II} + 3/2\ H_2O_2 \rightarrow Mn^{III}Mn^{IV}(\mu\text{-}O)_2 + H_2O + H^+ \quad (1)$$

In contrast, for **2a**, a single H_2O_2 molecule is needed but two H^+ ions are released [Equation (2)].

$$Mn^{II}Mn^{III} + H_2O_2 \rightarrow Mn^{III}Mn^{IV}(\mu\text{-}O)_2 + 2\ H^+ \quad (2)$$

The increased acidity of the medium may be responsible for the higher proportion of the precursor species.

Here we have shown that complexes **1a**, **1b** and **2a** are able to disproportionate 100% of the initial hydrogen peroxide in acetonitrile or methanol solution by means of a first-order reaction with respect to catalyst and hydrogen peroxide. This observation departs from the results of Okawa[13,28] who claimed that the complexes of dissymmetric pentadentate imine/amine-phenolato ligands are able to disproportionate only 65% of the initial hydrogen peroxide, while the symmetric ones disproportionate all the hydrogen peroxide. Nevertheless, the present hexadentate amine ligands and probably also the heptadentate ligand used by Nishida[25] appear flexible enough to accommodate the bis(μ-oxo)dimanganese(III,IV) cores by allowing a phenolate shift which frees some coordination position.[21] Such a situation may not be easily achievable with more conjugated ligands involving imine donors. When the dioxygen evolution rates are compared, our best catalyst (**2a**) is around 9 times more active than the comparable phenolato-bridged complexes described in the literature (after converting initial rates to the same conditions).[13,25] Nevertheless, they appear much less active than the dimanganese(II,II) complexes of tripodal ligands recently reported.[29]

Conclusions

The present kinetic and thermodynamic studies fully support our initial mechanistic investigations of the catalase-like reaction by dimanganese(II,II) complexes. A unique mechanism seems to be operative which is based on shuttling between a (μ-oxo)dimanganese(II,III) and a bis(μ-oxo)dimanganese(III,IV) species. This illustrates the fact that to efficiently disproportionate H_2O_2 the system uses the Mn_2 pairs, the redox potentials of which are the most adapted whatever the initial oxidation states of the Mn ions. The systems differ by the initiation process required to enter the catalytic cycle and the sensitivity to protonation which appears to significantly alter the composition of the medium and the kinetics.

Experimental Section

General: All solvents and reagents were of the highest quality available and were used as received unless noted otherwise. The concentration of the hydrogen peroxide stock solution (30% w/w) was determined monthly by permanganate titration. The ligand HL was prepared according to the literature procedure.[22]

Syntheses: The complexes **1a**, **1b** and **2a** where synthesised according to the procedure described before.[20]

Caution: Perchloric acid and perchlorate salts are potentially dangerous and explosive and must be handled with care and in small quantities.

Spectroscopic Measurements: Electronic absorption spectra were recorded with a Hewlett Packard HP 89090A diode array spectrophotometer. Electrospray ionisation mass spectra were obtained with an LCQ Finnigan Thermoquest ESI source spectrometer with an ion trap and an octupolar analyser. EPR spectra at X band were recorded with an EMX Bruker spectrometer equipped with an Oxford Instruments cryostat ESR900. All spectra presented were recorded with the following set of conditions: T = 10 K, P = 0.2 mW, modulation F = 100 kHz, I = 9 G.

Kinetic Measurements: The rate determinations of the catalase-like reactions were performed by volumetric measurements of the evolved dioxygen. The whole apparatus, constructed from borosilicate glass, was kept at a constant temperature (±0.2 °C) using a thermostatted ethanol circulation bath (Haake FQ-4). In a standard procedure, catalyst solution (2 mL) was placed in the kinetic apparatus. The solution was stirred for 30 min to reach a stable temperature. The chosen volume of hydrogen peroxide stock solution was added and the volume of evolved dioxygen was then measured as a function of time. To compare the kinetics at different temperatures, the volume of the gas was converted to a reference temperature (273 K) using the ideal gas law. The volume was also corrected for the vapour pressure of the solvent at the working temperature using the expression $V_{corr} = V_{mes}*(P_{atm}–P_{vap})/P_{atm}$ where V_{corr} is the corrected volume, V_{mes} the measured volume,

P_{atm} the atmospheric pressure and P_{vap} the vapour pressure of the solvent at the working temperature. In most cases, the initial rates were obtained by measuring the slopes of the tangents of the curve $v(O_2)$ vs. time at 0 s. When a lag phase was present (i.e. experiments with **1a** at low H_2O_2 concentrations), the largest slope after the initiation phase was used.

[1] B. Halliwell, J. M. C. Gutteridge, *Meth. Enzymol.*, Academic Press, San Diego, **1990**.
[2] E. R. Stadtman, P. B. Berlett, P. B. Chock, *Proc. Natl. Acad. Sci. USA* **1990**, *87*, 384–388.
[3] Y. Kono, I. Fridovich, *J. Biol. Chem.* **1983**, *258*, 6015–6019.
[4] G. S. Allgood, J. J. Perry, *J. Bacteriol.* **1986**, *168*, 563–567.
[5] V. V. Barynin, A. I. Grebenko, *Dokl. Akad. Nauk SSSR* **1986**, *286*, 461–464.
[6] G. C. Dismukes, *Chem. Rev.* **1996**, *96*, 2909–2926.
[7] A. Wu, J. E. Penner-Hahn, V. L. Pecoraro, *Chem. Rev.* **2004**, *104*, 903–938.
[8] S. V. Antonyuk, V. R. Melik-Adamyan, A. N. Popov, V. S. Lamzin, P. D. Hempstead, P. M. Harrison, P. J. Artymyuk, V. V. Barynin, *Crystallogr. Rep.* **2000**, *45*, 105–116.
[9] V. V. Barynin, M. M. Whittaker, S. V. Antonyuk, V. S. Lamzin, P. M. Harrison, P. J. Artymiuk, J. Whittaker, *Structure* **2001**, *9*, 725–738.
[10] S. V. Khangulov, V. V. Barynin, S. V. Antonyuk-Barynina, *Biochim. Biophys. Acta* **1990**, *1020*, 25–33.
[11] G. S. Waldo, J. E. Penner-Hahn, *Biochemistry* **1995**, *34*, 1507–1512.
[12] V. L. Pecoraro, M. J. Baldwin, A. Gelasco, *Chem. Rev.* **1994**, *94*, 807–826.
[13] H. Okawa, H. Sakiyama, *Pure Appl. Chem.* **1995**, *67*, 273–280.
[14] A. E. M. Boelrijk, G. C. Dismukes, *Inorg. Chem.* **2000**, *39*, 3020–3028.
[15] A. Gelasco, S. Bensiek, V. L. Pecoraro, *Inorg. Chem.* **1998**, *37*, 3301–3309.
[16] H. Wada, K. I. Motoda, M. Ohba, H. Sakiyama, N. Matsumoto, H. Okawa, *Bull. Chem. Soc. Jpn.* **1995**, *68*, 1105–1114.
[17] H. Sakiyama, H. Okawa, R. Isobe, *J. Chem. Soc., Chem. Commun.* **1993**, 882–884.
[18] Y. Sasaki, T. Akamatsu, K. Tsuchiya, S. Ohba, M. Sakamoto, Y. Nishida, *Polyhedron* **1998**, *17*, 235–242.
[19] I. Romero, M.-N. Collomb, A. Deronzier, L. Dubois, J.-M. Latour, J. Pécaut, *Inorg. Chem.* **2002**, *41*, 1795–1806.
[20] L. Dubois, D.-F. Xiang, X.-S. Tan, J. Pécaut, P. Jones, S. Baudron, L. Le Pape, J.-M. Latour, C. Baffert, S. Chardon-Noblat, M.-N. Collomb, A. Deronzier, *Inorg Chem.* **2003**, *42*, 750–760.
[21] L. Dubois, R. Caspar, L. Jacquamet, P.-E. Petit, M.-F. Charlot, C. Baffert, M.-N. Collomb, A. Deronzier, J.-M. Latour, *Inorg. Chem.* **2003**, *42*, 4817–4827.
[22] W. Kanda, W. Moneta, M. Bardet, E. Bernard, N. Debaecker, J. Laugier, A. Bousseksou, S. Chardon-Noblat, J. M. Latour, *Angew. Chem. Int. Ed. Engl.* **1995**, *34*, 588–590.
[23] T. Nakamura, K. Niwa, S. Usugi, H. Asada, M. Fujiwara, T. Matsushita, *Polyhedron* **2001**, *20*, 191–201.
[24] C. Palopoli, B. Chansou, J. P. Tuchagues, S. Signorella, *Inorg. Chem.* **2000**, 1458–1462.
[25] Y. Nishida, T. Akamatsu, K. K. Tsuchia, M. Sakamoto, *Polyhedron* **1994**, *13*, 2251–2254.
[26] D. R. Gamelin, M. L. Kirk, T. L. Stemmler, S. Pal, W. H. Armstrong, J. E. Penner-Hahn, E. I. Solomon, *J. Am. Chem. Soc.* **1994**, *116*, 2392–2399.
[27] C. Higuchi, H. Sakiyama, H. Okawa, R. Isobe, D. E. Fenton, *J. Chem. Soc. Dalton Trans.* **1994**, 1097–1103.
[28] C. Higuchi, H. Sakiyama, H. Okawa, D. E. Fenton, *J. Chem. Soc. Dalton Trans.* **1995**, 4015–4020.
[29] M. U. Triller, W.-Y. Hsieh, V. L. Pecoraro, A. Rompel, B. Krebs, *Inorg. Chem.* **2002**, *41*, 5544–5554.

Received: September 24, 2004

